



An integrated approach of reservoir characterization of Y gas field in Central Bredasdorp Basin, South Africa

Rotondwa Masindi¹ · K. B. Trivedi² · M. Opuwari¹

Received: 13 November 2021 / Accepted: 20 January 2022 / Published online: 15 February 2022
© The Author(s) 2022

Abstract

The study attempts to address the knowledge gap in the Bredasdorp Basin Offshore South Africa by using newly acquired seismic data with an enhanced resolution, integrating core and well log to provide a solution. The main objective of this study was a volumetric sandstone reservoir characterization of the 13At1 and 10At1 sandstones deposited in the upper shallow marine environment. The results reveal four facies grouped as facies 1 (claystone), facies 2 (intercalation of claystone and sandstone), facies 3 (medium sandstone), and facies 4 (fine-medium sandstone grain deposited in a deep marine environment). Facies 3, the medium-grained sandstone, has the best reservoir quality rock, while facies 1, which is predominantly claystone, has the least rock quality. The study has produced a calculated volume of gas in the 10At1 sand (upper and lower sand is 30.01 billion cubic feet (bcf)) higher than that of the 13At1 sand (27.22 bcf of gas). Improved seismic resolution enhanced the accuracy of results. It is advisable to focus further field development in the eastern part of the Y gas field because of good reservoir quality and production developed due to the sand in the 10At1 sequence.

Keywords Facies · Volume in place · Deep marine environment · 13AT1 · 10AT1 · South Africa

Introduction

The pursuit for the accumulation of hydrocarbons required an advance comprehensive approach to expedite exploration, appraisal, development and production activities (Evans et al. 2019). However, the capability to sufficiently characterize reservoirs remains a critical challenge. It is vital to use dependable reservoir characterization approaches for an effective and reliable reservoir delineation and description. The reservoir zonation approach is one of the methods used by researchers to understand the internal architecture and factors controlling flow zones in a reservoir (Nabawy and Al-Azazi 2015; Nabawy and ElHariri 2008; Opuwari et al. 2019; M. Opuwari et al. 2020a, b; Radwan et al. 2020). The reservoir zonation approach helps to understand reservoir heterogeneity and identify productive zones within a

reservoir, which is subsequently upscale to field-scale reservoir mapping (Opuwari 2010; Qassamipour et al. 2021).

Several case studies using core, seismic, and wireline log data have been effectively applied in reservoir characterization to explore and develop hydrocarbon (Das and Chatterjee 2018; Gogoi and Chatterjee 2019; Gupta et al. 2012; Nabawy et al. 2018; Neely et al. 2021; Sohail et al. 2020; Teama et al. 2019; Verwer and Braaksma 2009). An enhanced classification of lithofacies and depositional environment centred on core, well log, and seismic data is important for formation evaluation, prospect identification and field development (Ashraf et al. 2019; Elamri and Opuwari 2016; Evans et al. 2019). The heterogeneity and the complex nature of reservoir properties can be effectively described and quantified by means of available core data, well log and seismic data (Gogoi and Chatterjee 2019).

The study area is the Y field (Fig. 1), which has three exploration wells (Y-01, Y-02, Y03) situated in the central Bredasdorp Basin offshore of South Africa (Brown 1995; McMillan et al. 1997). An additional exploration well (X-01) in Field X, approximately 6 km from the Y field, is used for broad correlation. The primary target of this study is in the Lower Cretaceous (Valaginian to Albian age) sediments

✉ M. Opuwari
mopuwari@uwc.ac.za

¹ Petroleum Geoscience Group, Earth Science Department, University of the Western Cape, Bellville 7535, Republic of South Africa

² Petroleum Oil and Gas Company of South Africa (PetroSA), 151 Franc Conradie Parow, Cape Town, South Africa

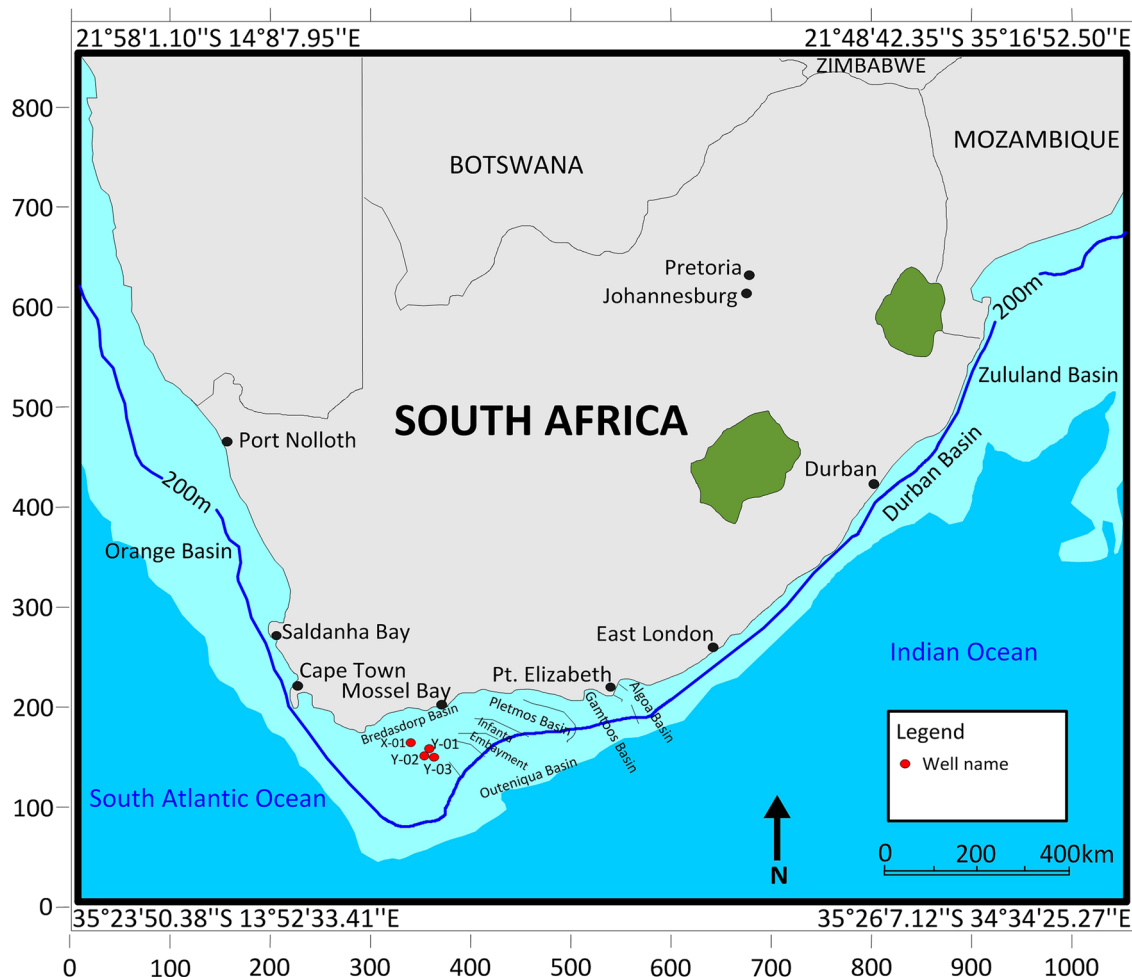


Fig. 1 Location map of study area showing wells used in this study in red circle

where hydrocarbon has been discovered within the 5At1 to 13At1 interval (Petroleum Agency 2003).

Extensive work has been done on the geology and petroleum system of the Bredasdorp Basin that is bounded by the southern Outeniqua basin, of which recent hydrocarbon was discovered. In one of those studies in the central Bredasdorp Basin, it was documented that some gas reservoirs are thin, which are cumbersome or unidentifiable on a seismic scale (Corbett et al. 2011; Grobblers 2005; Turner et al. 2000). Previous studies in the Bredasdorp Basin on reservoir characterization include (Baiyegunhi et al. 2020a, 2020b, 2020c; Barton 1997; Mudaly et al. 2009; Opuwari et al. 2020a, b; Opuwari et al. 2021; Saffou et al. 2020). Although there is an in-house study by an oil and gas company on the reservoir architecture description and characterization of the Bredasdorp Basin, there is still a gap in the published literature on comprehensive reservoir characterization of the central part of Bredasdorp Basin. Previous seismic data acquired in the study area have poor resolutions, making it challenging to create plausible geological models.

This study is to provide solution to this knowledge gap by using the newly acquired seismic data with an enhanced resolution, integrating core and well logs. The study has produced a calculated volume of gas in the 10At1 and 13At1 sand and identified areas to focus during further field development programme because of the good reservoir quality. Improved seismic resolution enhanced the accuracy of results. Consequently, this paper presents importance of an integrated approach to reservoir characterization.

Geological setting

The offshore basins of South Africa are grouped into three sections: the western section comprises the Orange Basin, the Eastern area (Zululand and Durban Basins), and the Southern region (Outeniqua Basin), as shown in Fig. 1. The Outeniqua Basin, which is the focus of this study, was formed earlier than the west and east Gondwana separation and stretched on the Falkland plateau (Jungslager 1999;

Roux 2000). There are four sub-basins in the Outeniqua basin known as the Bredasdorp (study area), Gamtoos, Pletmos and Algoa. According to Miall (1980), the Southern offshore basins exhibit rift basins with normal faults and half grabens.

Rifting in Southern Africa is postulated to begin during the middle to the late Jurassic period (Boada et al. 2001; McMillan et al. 1997). The rifting that occurred created normal faults (Roux 1997). The sediments that have mostly filled the Bredasdorp Basin are marine sediments deposited in the Late Jurassic to Early Cretaceous fluvial and shallow marine deposits of the Aptian to the Maastrichtian age (Grobler 2005; Turner et al. 2000), presented in Fig. 2.

During the mid-Jurassic to the Valanginian, synrift I was manifested from the basement to the 1At1 unconformity (Fig. 2). Rifting initially was due to horst and graben structures characteristic of extensional tectonics (Elliott 1997; McMillan et al. 1997). In the Late Valanginian to the Hauterivian, 1–6At1 sequence boundary is observed, which depict the synrift II phase, characterized by swift subsidence and extensive flooding (Van der Spuy 2003). The 6–13At1 sequence boundary is observed in the transitional early drift phase at Hauterivian to the Aptian. In the early Aptian, there was a decline in subsidence rates and faulting, resulting in a more stable Bredasdorp Basin (Petroleum Agency 2003). The drift phase occurred at the Albian to Maastrichtian time which is the 13–22At1.

Most oil and gas source rocks are shales in the central Bredasdorp Basin, positioned among the transitional period in deep marine, transgressive, and early highstand tracts of the synrift I (Fig. 2). The sandstone reservoirs in the central Bredasdorp Basin are predominantly upper shallow marine (USM) depositional environment. The upper shallow marine sandstones are the best gas reservoirs and have good porosities and permeability (Broad et al. 2006).

Data and methods

The Petroleum oil and gas company of South Africa (PetroSA) and the Petroleum Agency of South Africa (PASA) provided the data set used in this study. The data set provided includes suites of conventional wireline logs (gamma-ray, calliper, density, sonic, neutron, and resistivity), seismic data (2D and 3D lines), core data, conventional and special core analysis reports, and well completion report. Schlumberger Petrel and Sedlog software packages were used for data analysis and interpretation.

Two of the wells used (Y-01 and Y-02) had core data laid out and watered to observe the grain size and structural features. This process was accompanied by a recording of lithology description of the core to establish sedimentology parameters such as grain size distribution, structure and

lithofacies distribution. The cores were photographed, and the recorded data from the core evaluation were exported to Sedlog software. A project was created in Petrel, and the various data sets obtained were loaded in their different formats before quality check and control were performed. Quality control and data editing were done to improve data quality where necessary and used for analysis and interpretation.

For petrophysical evaluation and stratigraphy modelling, a wireline log was integrated with core and seismic data. Stratigraphic modelling allows the determination of similar rock bodies at different locations where well data are available. The petrophysical evaluation process commences with the estimation of reservoir parameters, followed by determining the volume of clay, total and effective porosity, water saturation, and permeability estimation using core facies as a guide.

The volume of clay (Vcl) was determined from the GR log by calculating the gamma-ray index using the equation developed by Altas (1979), and Fertl and Frost (1980), as follows:

$$\text{GRI} = \frac{\text{Vcl} = \text{Gr}(\log) - \text{Gr}(\min)}{\text{Gr}(\max) - \text{Gr}(\min)} \quad (1)$$

where Gr (log) = Gamma-ray log value of formation to be evaluated, Gr (min) = Minimum value of gamma-ray reading on a clean formation, Gr (max) = Maximum gamma ray reading. For a clean sand interval, calculated Vcl ≤ 10%; for a shaly interval, Vcl is between 10 and 35%; and for a shaly interval, Vcl ≥ 35% (Opuwari 2010).

Porosity was determined from the density log using the following relationships of Asquith and Gibson (1982) as follows;

$$\text{Porosity} = \frac{\rho_{\max} - \rho_b}{\rho_{\max} - \rho_f} \quad (2)$$

where ρmax = Matrix density determined from core, ρb = Bulk density, ρf = Fluid density.

The effective porosity was determined by correcting the effect of shale on porosity using the following equation:

$$\text{Effective porosity} = \frac{(\rho_{\max} - \rho_b) - \text{Vcl}(\rho_{\max} - \rho_{cl})}{(\rho_{\max} - \rho_f) - (\rho_{\max} - \rho_f)} \quad (3)$$

where ρcl = Density of clay.

The Indonesia water saturation (SWIndonesia) equation proposed by Poupon-Leveaux (1971) calculated water saturation. The equation is provided below:

The empirical relationship can be written as follows:

$$\text{Swind} = \left(1/\sqrt{Rt} = \frac{\sqrt{\Phi e^m}}{a \cdot R_w} + \frac{\text{Vcl}^{(1-\text{Vcl}/2)}}{\sqrt{R_{cl}}} \times \text{Sw}^{n/2} \right) \quad (4)$$

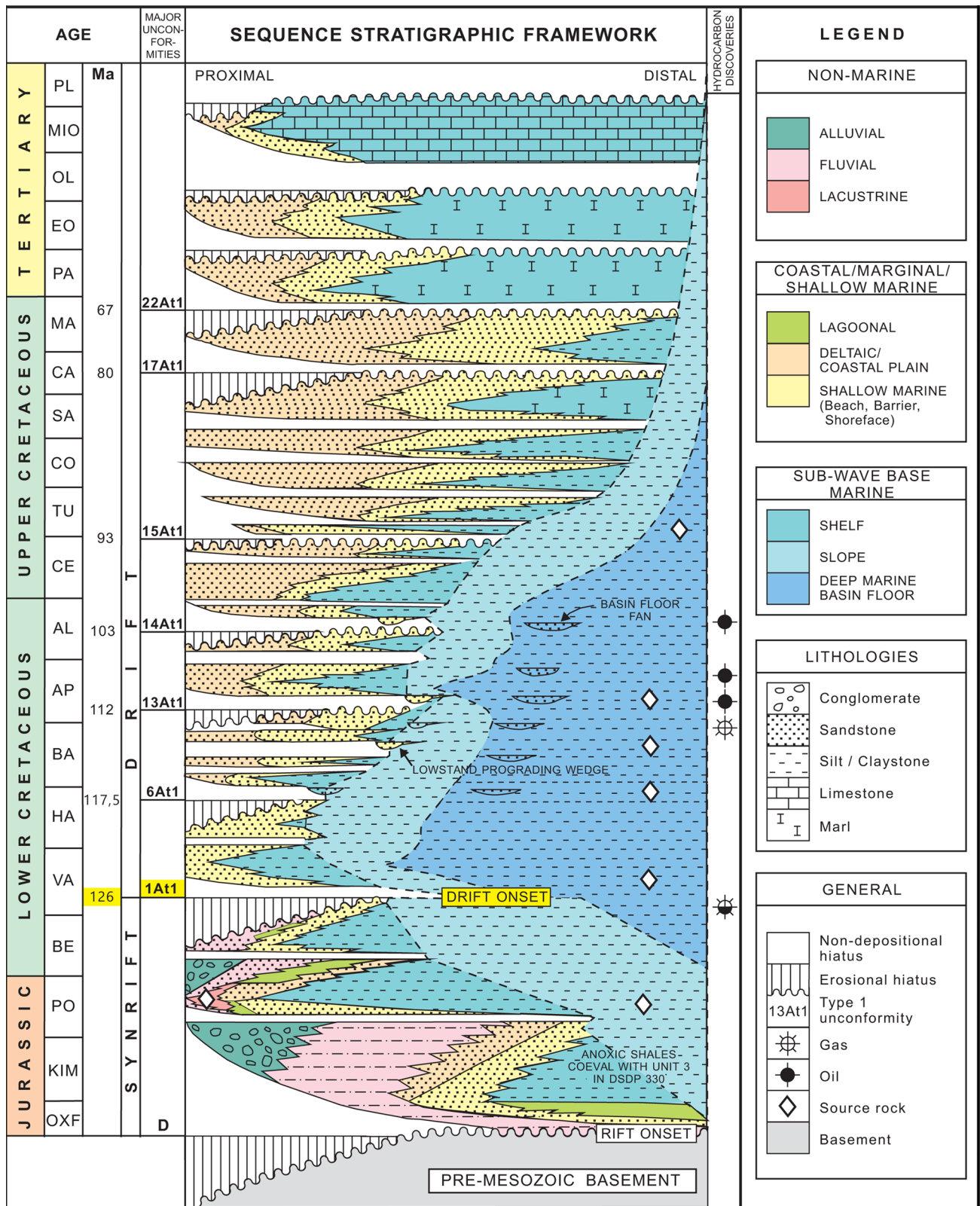


Fig. 2 Chronostratigraphic chart of the Bredasdorp Basin

where R_t = Resistivity curve from log, R_{cl} = Resistivity of wet clay, Φ_e = Effective porosity calculated from Eq. 3. $Swind$ = Water saturation, fraction, V_{cl} = Volume of shale, fraction. R_w = Formation water resistivity. m = Cementation exponent. a = Tortuosity factor. n = Saturation exponent.

A relationship obtained from the cross-plot of core permeability against porosity was used to determine the permeability from the log as follows:

$$\text{Permeability} = 1.146 * \Phi_d^{0.67} (R^2 = 0.93) \quad (5)$$

where Φ_d = Porosity from density log.

The seismic interpretation process commenced with seismic to wireline log tie, Mistie adjustment, then unconformities identification, faults picking and horizon mapping.

Various surfaces and models were created in the workflow that culminates into the volumetric calculation. The reservoirs were delineated using the properties in a 3D grid, and the gas water contact (GWC) was also established. The flowchart of the study is presented in Fig. 3.

Results and discussion

Core analysis

The result of the core logging revealed four distinct lithofacies (Fig. 4) classified as follows:

Facies 1: Greyish black, fine-grained claystone, well sorted and laminated.

Facies 2: Intercalation of claystone and fine sandstone, fair sorting, claystone laminated.

Facies 3: Grey, massive sandstone, medium-grained, fair sorting, coarsening upward sequence.

Facies 4: Grey, fine to medium grain, fair sorting, sandstone interbedded with clay, coarsening upward sequence.

The four classified lithofacies are present in all the studied wells. Facies 1, predominantly of claystone, has the lowest rock quality and dominates in the upper part of the wells between 14 and 13A, intercalated with fine sandstone at intervals (Fig. 4). Facies 4 and 3 have the best rock quality with a reasonable thickness in all the well, bounded at the top and bottom by facies 1.

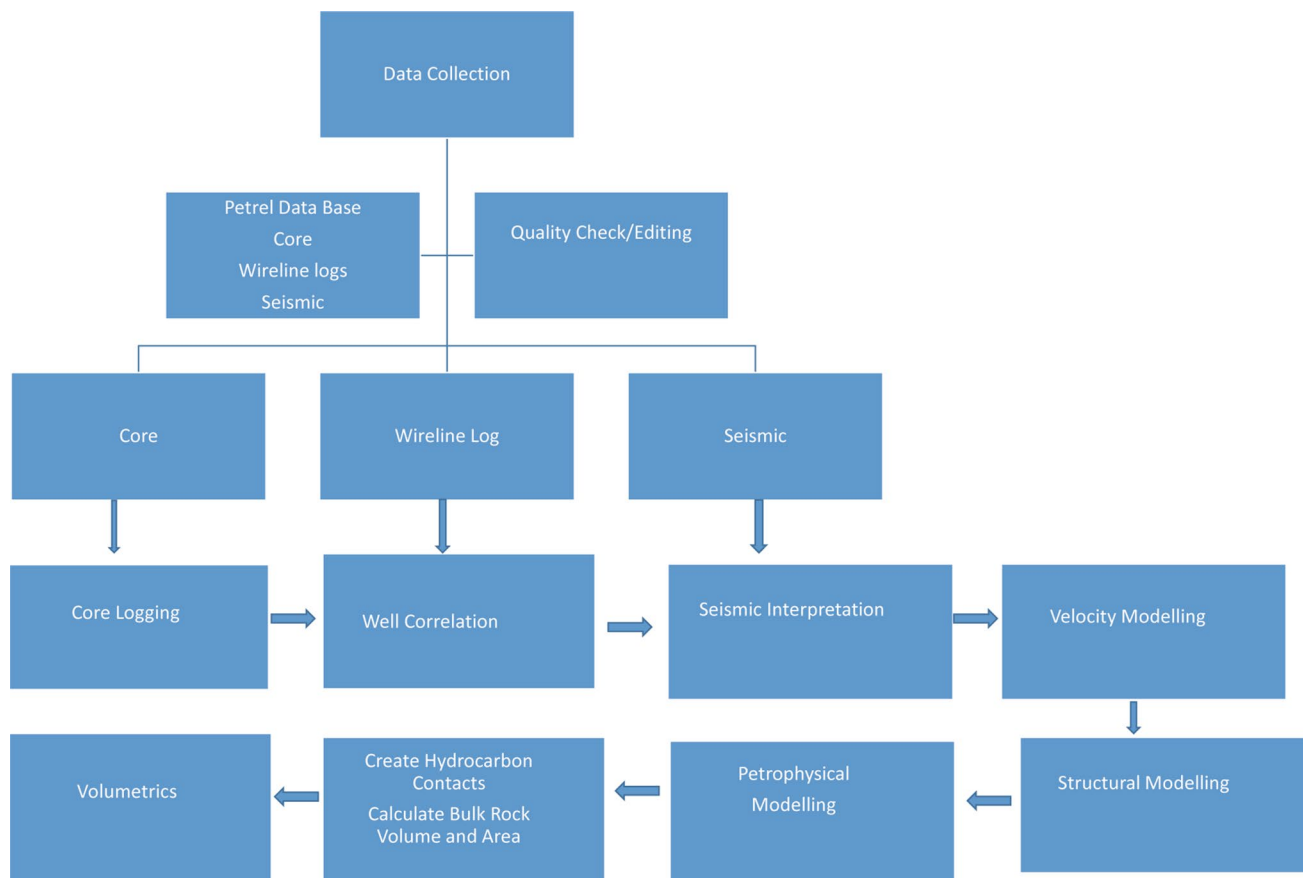


Fig. 3 Flow chart of study

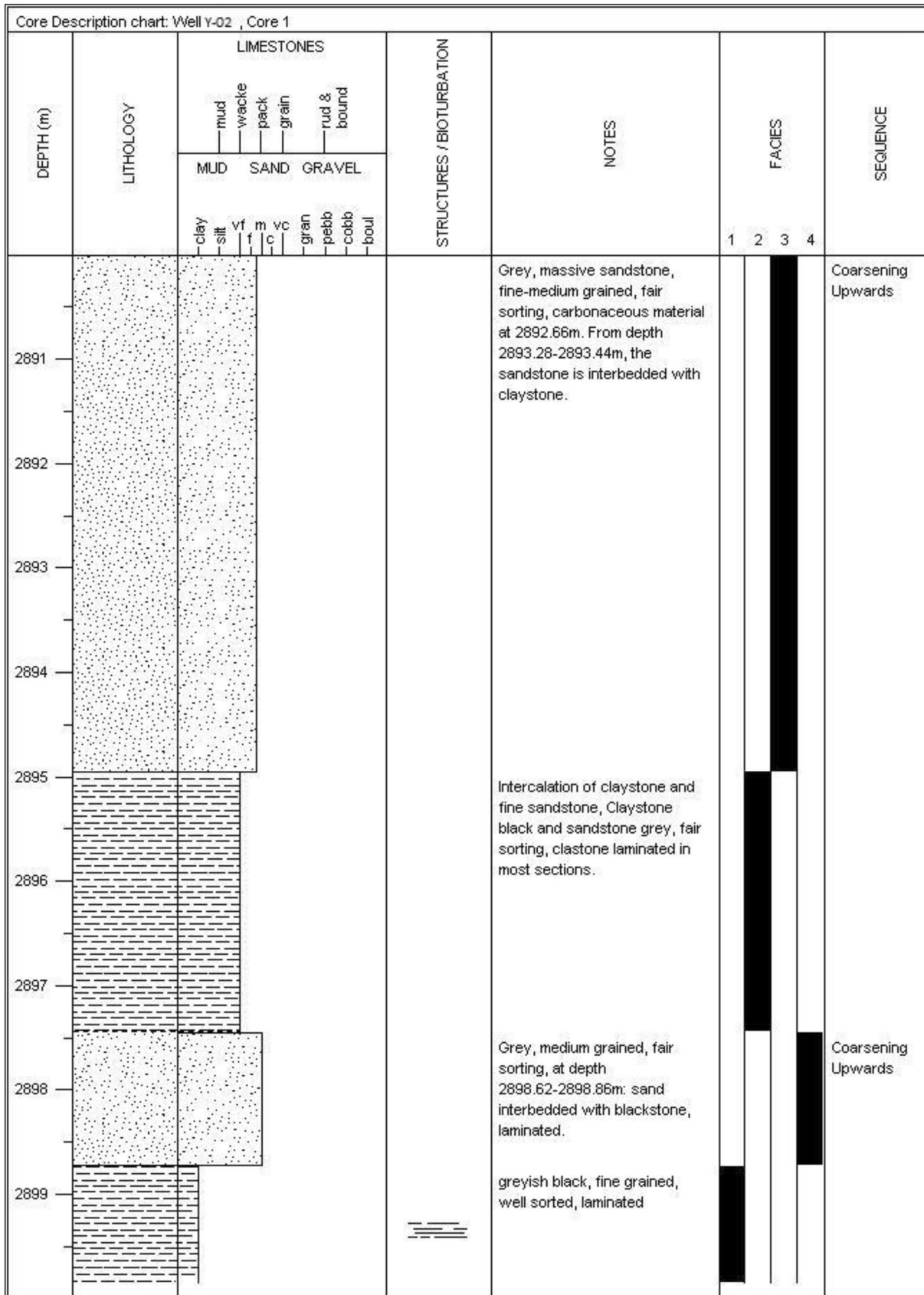


Fig. 4 Result of core logging showing four lithofacies

Well correlation

The lithostratigraphy correlation of the geological horizons based on the gamma-ray log is presented in Fig. 5. A baseline of 75 American Petroleum Institute (API) units was used to differentiate between a sandstone interval (0-75API) and a shale interval (75-150API). The top (at depth 2849 m) and bottom (at depth 2856 m) of horizon 13AT1 sandstones were correlated. The 13At1 sandstone has similar thicknesses throughout the three wells in the field.

Below the 13At1 sandstone is the 10At1 sandstone (from about 2898 m as top, to about 2955 m as base). Three key reservoir sandstone units were identified between the top (marker 10At1) and bottom (marker 10At1) of 10At1 sandstone in the studied well. The 10At1 horizon represents the base of the 10At1 sandstone. Well Y-01 has similar sandstone bodies to well Y-03. The sandstone bodies are thicker in well Y-01 than Y-02, and lower gamma-ray values are displayed in these sandstone bodies.

Facies modelling was performed from the gamma-ray log using the following criteria:

- Facies 1: 75–150 API.
- Facies 2: 25-75API.
- Facies 3: 0–15 API.
- Facies 4: 15-25API.

Due to the heterogeneity observed in the sediments, a layering operation was performed to incorporate the very fine sandstones found between the claystone and the intercalation of facies. The layering method resamples the facies data into 3D cells, takes the dominant facies in the pre-selected interval, and assigns it to the cell penetrated by the well (Puskarczyk 2020). The results of the facies layering method are compared to the core identified facies of the wells which are presented in track 5 of the wells (Fig. 6). The upscaled facies obtained from the layering method matches the core facies. Facies are important in reservoir modelling because the petrophysical properties are often highly correlated with facies types. Knowledge of facies constrains the range of variability in reservoir properties such as porosity, permeability, and saturation (Elamri and Opuwari 2016; Magoba and Opuwari 2017).

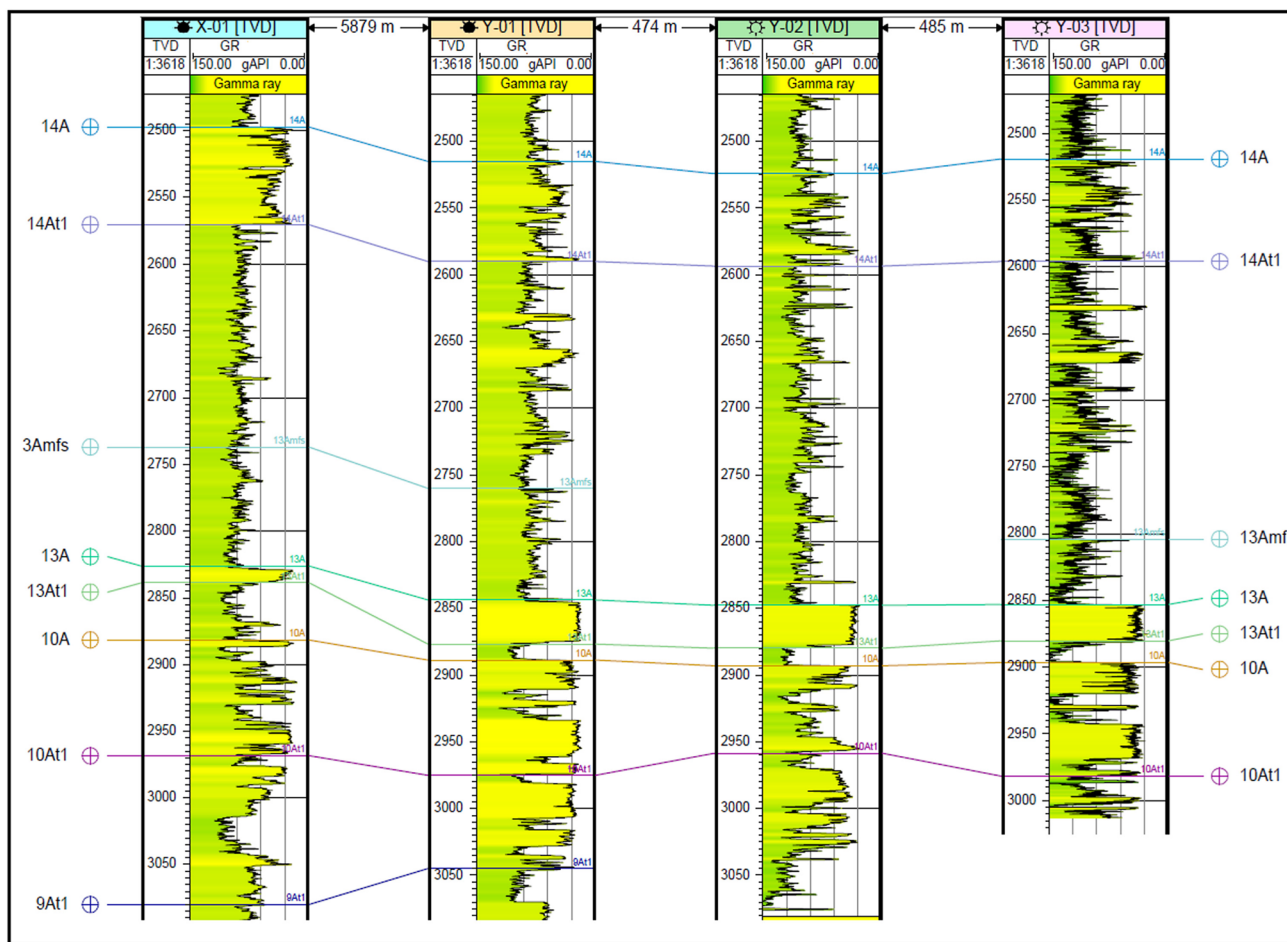


Fig. 5 Correlation of geological horizons based on gamma ray log

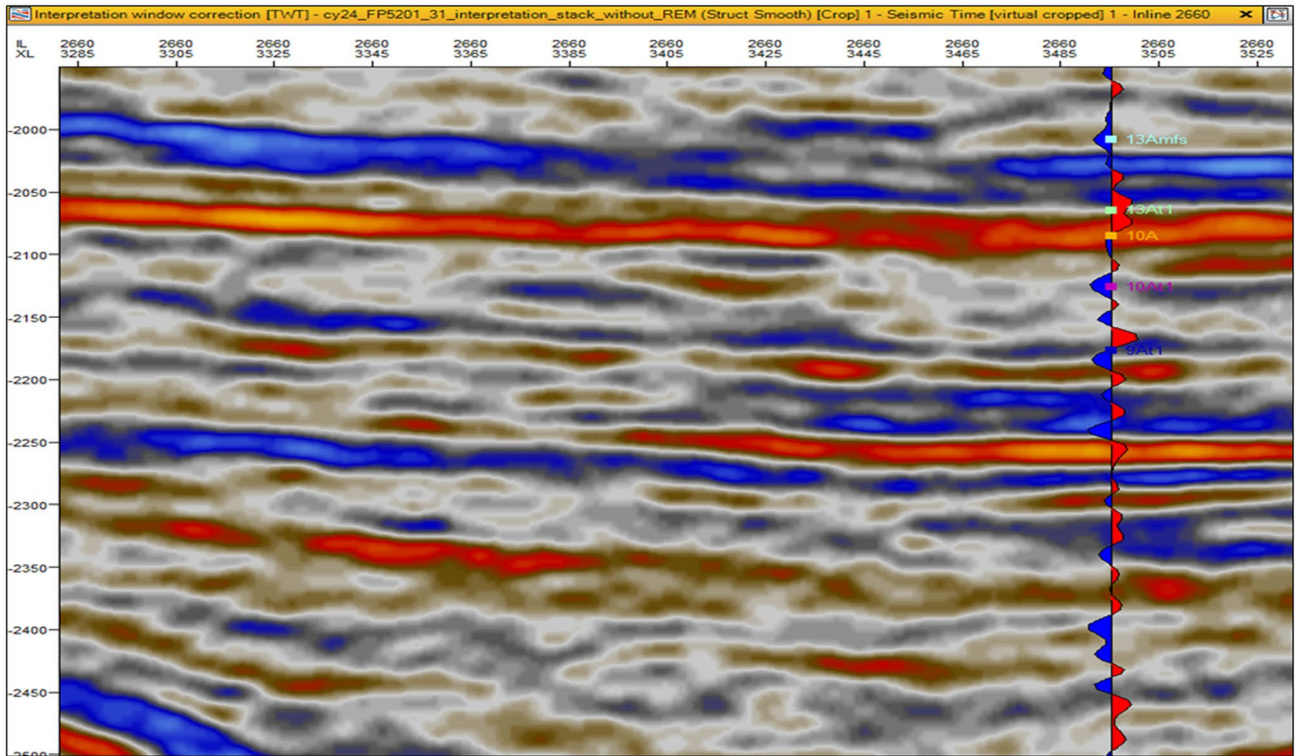


Fig. 7 Example of a seismic well tie for well Y-01 showing seismic log traces

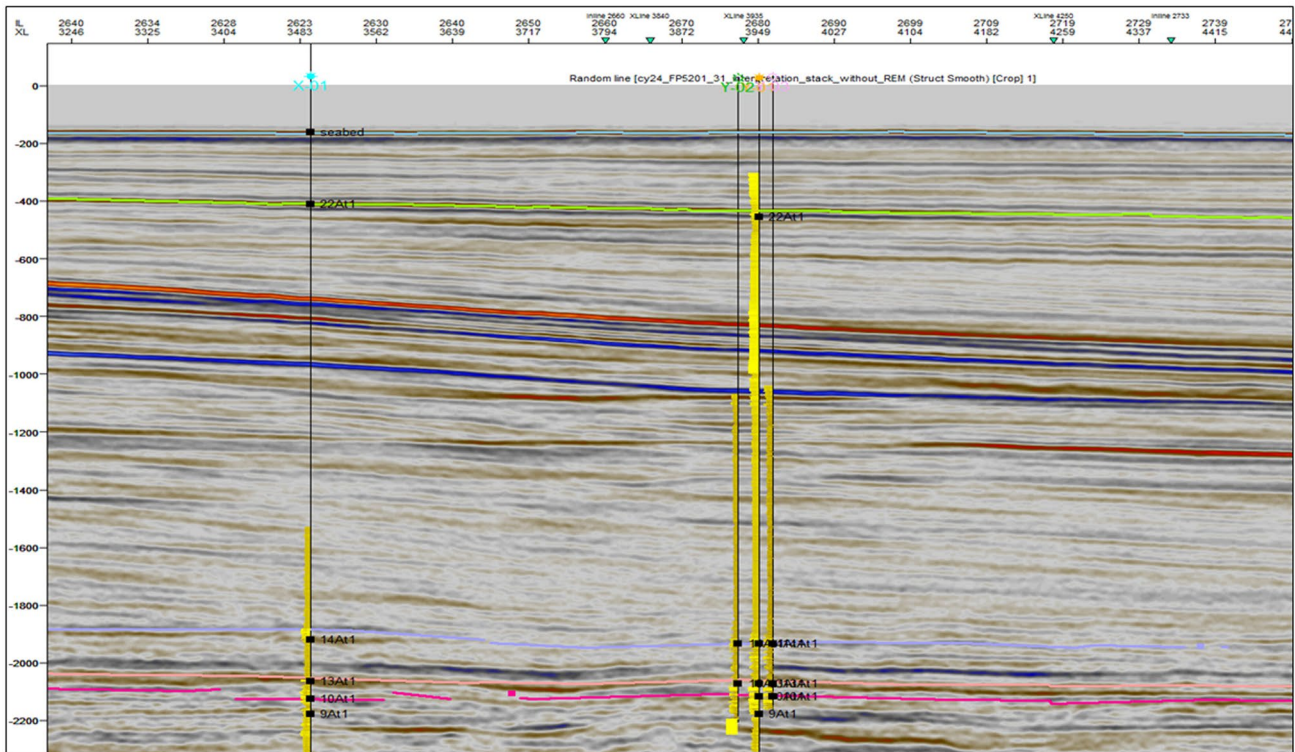


Fig. 8 Random lines show seismic section with mapped horizons from 22 to 10A11

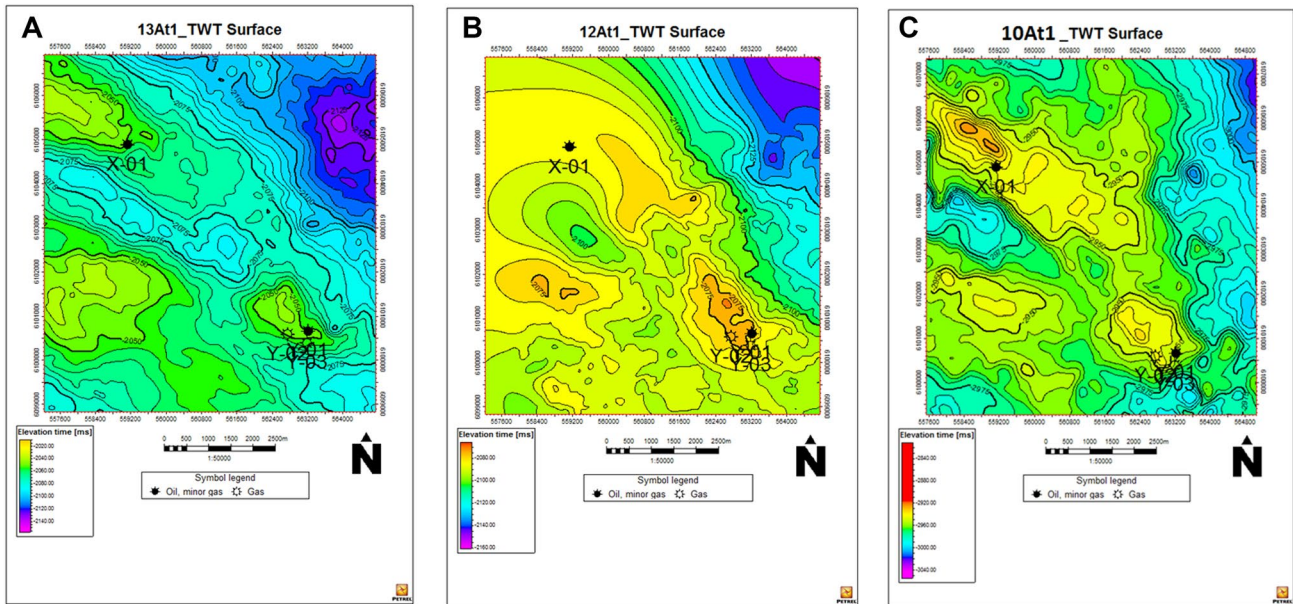


Fig. 9 Results of created two-way time (TWT) surfaces

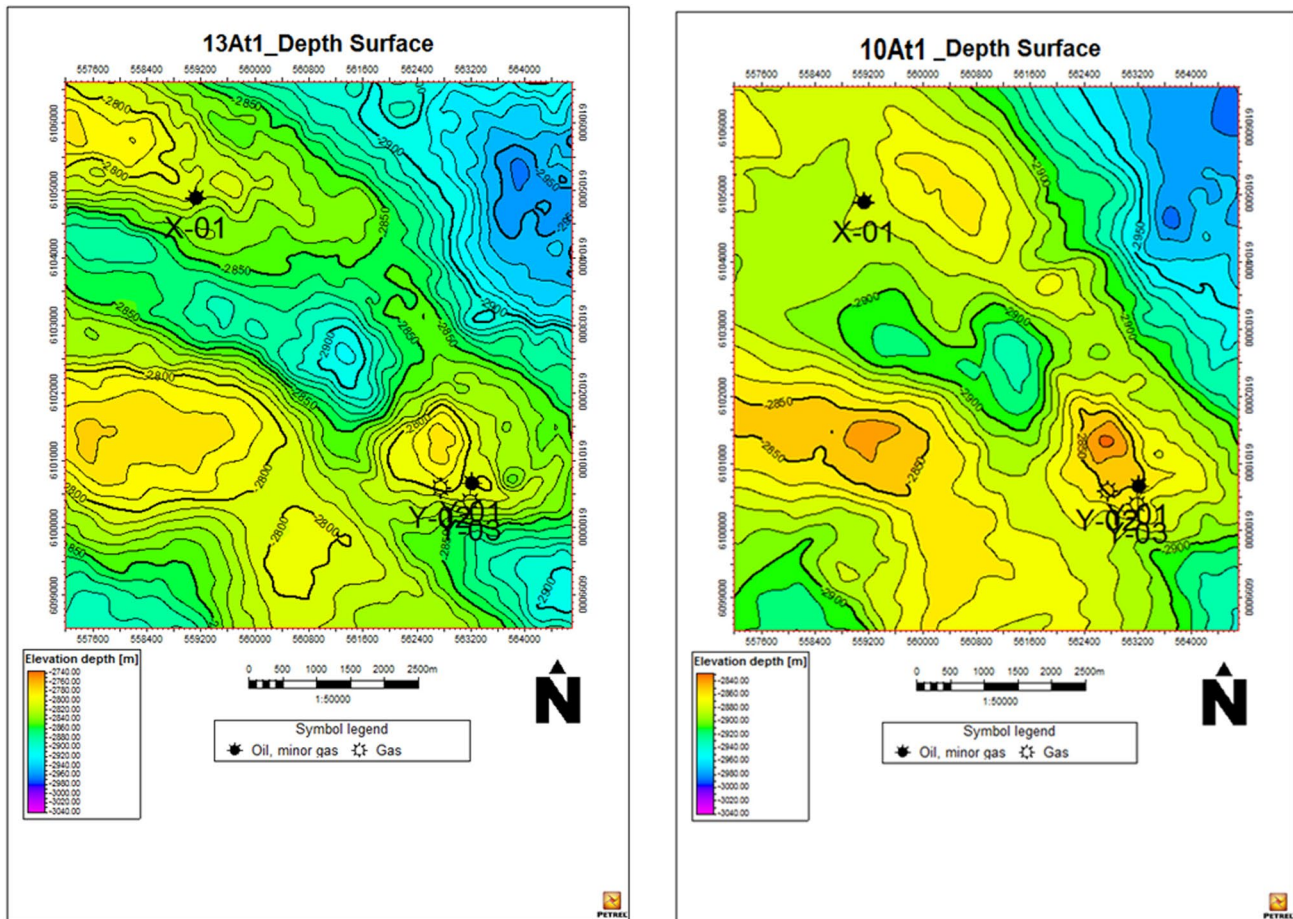
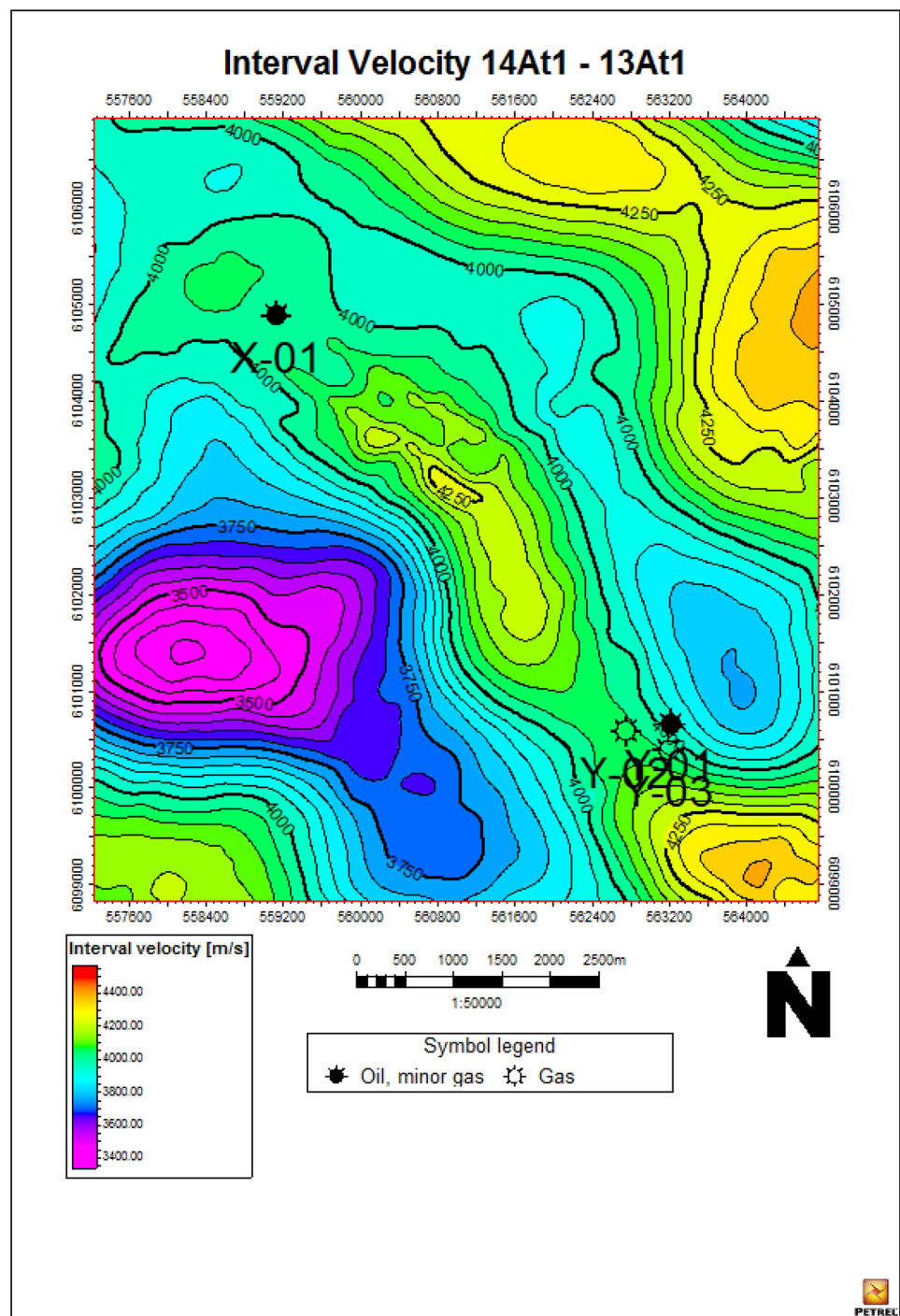


Fig. 10 Results of depth models for 13At1 and 10At1

Fig. 11 Results of velocity model for horizon 13At1 and 10At1

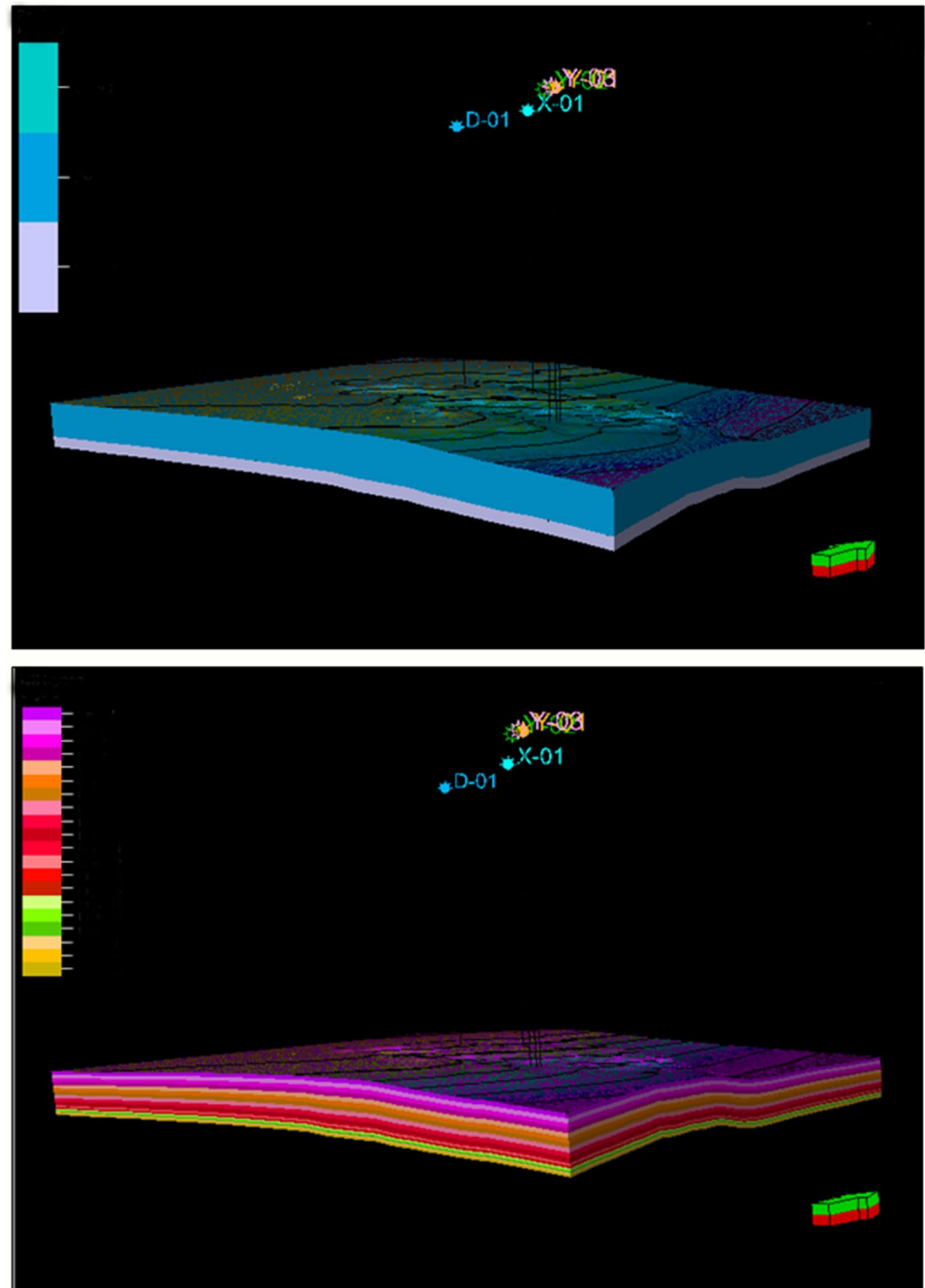


2 (between the 13 and 10At1 surfaces that represents the 10At1 sandstone). Zone 2 appears to be much thicker than zone 1. Further investigation of the two zones by the layering method produces a detailed surface geometry, showing a fill structure (Fig. 12b). The results of the petrophysical models populated in a created structural grid are presented in the next section.

Volume calculation and uncertainty analysis

Continuous variables with spatial correlation, such as porosity, were populated stochastically using sequential Gaussian simulation (SGS) algorithm conditioned to the facies model using Petrel Software. Data analysis and transformation were performed as it is the main prerequisite to run

Fig. 12 Structural grid results



the petrophysical modelling. Firstly, log-scale porosity was scaled-up, and quality checked into the pre-defined layers.

Effective porosity curve derived from petrophysical interpretation was used as input data for the porosity model. Statistical analysis of the porosity, permeability, and water saturation log data was performed, upscaled, and populated in the grid created earlier to produce a property model. Results of the upscaled values are presented in Table 1, while the distribution of porosity and facies is shown in Fig. 13a, b, and permeability

Table 1 Results of the upscale petrophysical properties

Sequence	Property	
	Porosity %	Permeability mD
13A Sands	8–10	85–90
10A Sands upper	7–8	0.5–90
10A Sands lower	5–7	0.5–70

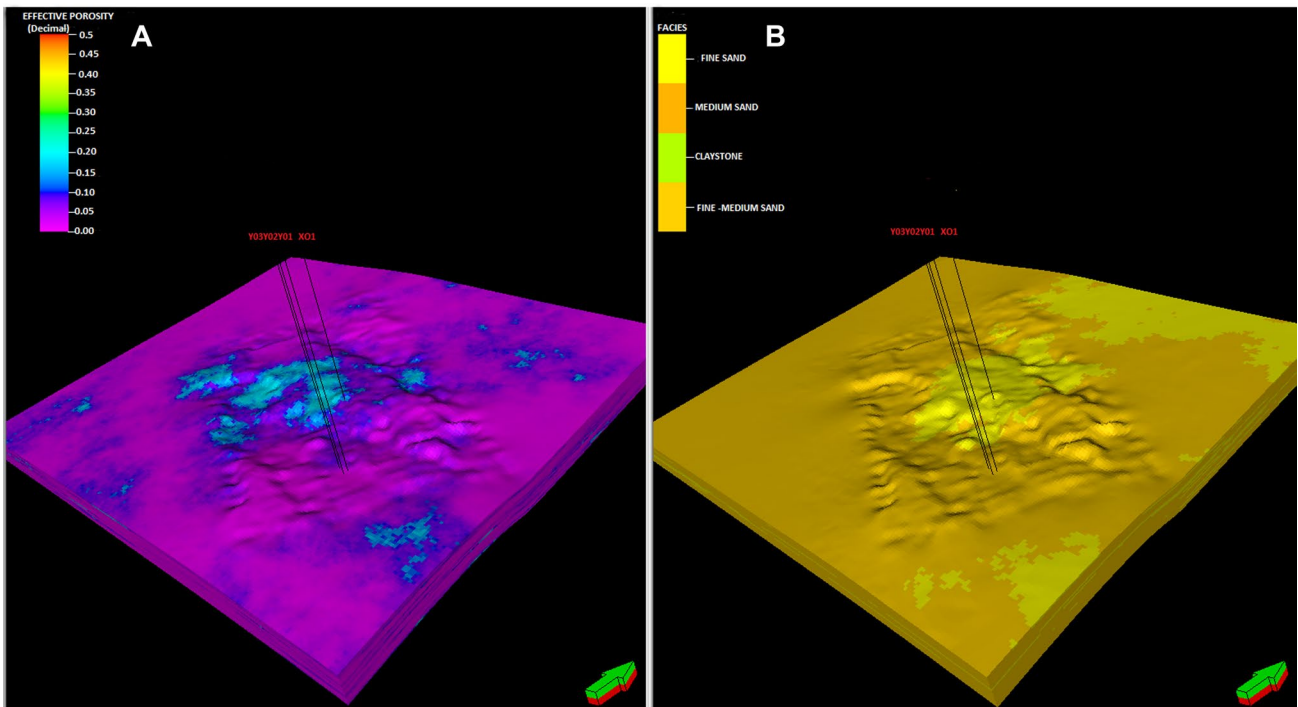


Fig. 13 a, b Distribution of porosity property and facies

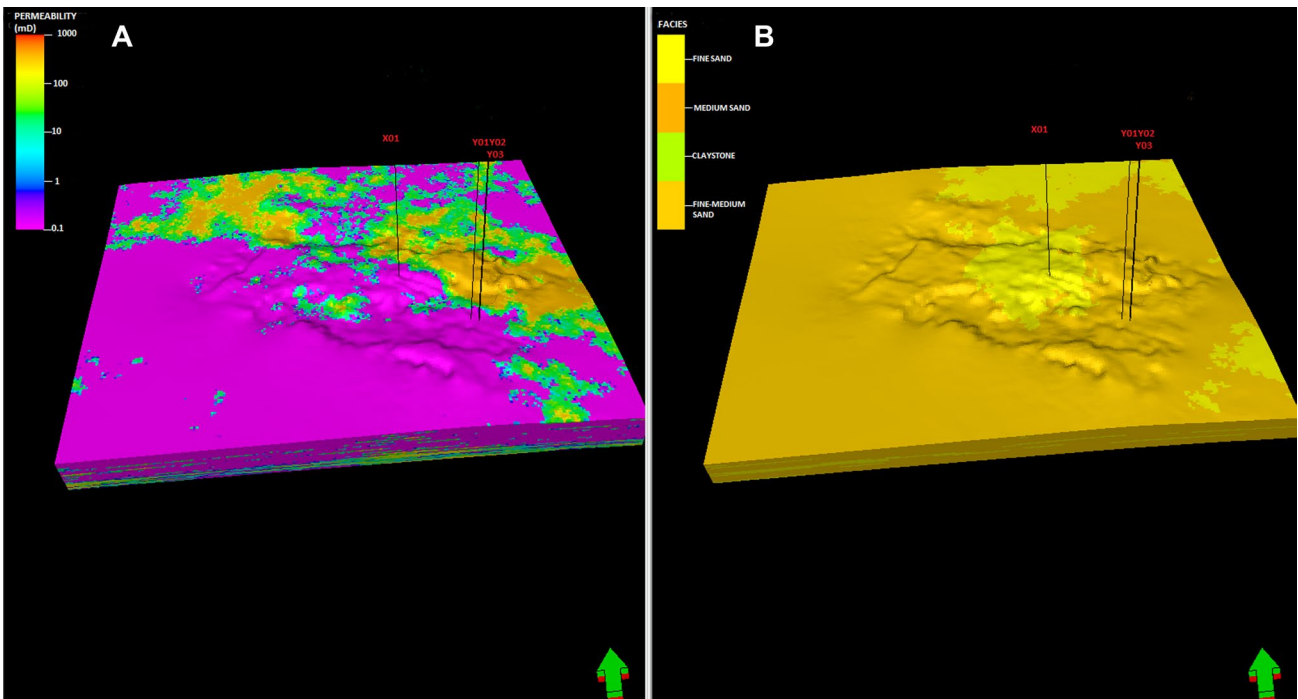


Fig. 14 a, b Results of the distribution of permeability with facies

and facies model is shown in Fig. 14a, b. The properties models are done conditioned to facies, to have a match between property values and facies. Comparison of property model

with facies showed that facies 1, predominantly claystone, have low porosity and permeability values in Figs. 13 and 14. Conversely, sandstone exhibits higher porosity and permeability

values. The porosity data of the field of study range between 5 and 12%. It is observed that facies 4 has the highest porosity values. The permeability surface model result (Fig. 14b) shows that the upper sequence (13At1 sand and above) of the formation has lower permeability values (0.5–10mD) in comparison to the lower sequence (10At1 sand) with permeability values ranging from 0.5 to 90mD. These high permeability values exhibited at 10At1 sand indicate well-connected pore spaces that will enhance reservoir performance (Opuwari et al. 2021, Goigo and Chatterjee 2019; Mondal and Chatterjee 2021). The water saturation models (Fig. 15a, b) with facies were executed separately for the 13At1 sandstone and Fig. 15c, f for 10At1 sandstone because they have different gas water contacts (GWCs). Figure 15a, which reveal fair to high water saturation between 40 and 80%. High water saturation is observed in the western side of the field of study, and a decline is observed towards the east.

Within the 10At1 sandstone, low to fair water saturation (40–65%) is revealed (Fig. 15c, e) for the upper and lower 10At1 sand. The 10At1 sandstone shows water saturation ranging between 40 and 60%, which indicates the high deliverable of hydrocarbon in this sandstone. Similarly, the 10At1 sandstone model shows that the water saturation is higher at the western side of the field and lower at the eastern side of the field. A comparison of water saturation values for the different sequences showed that the claystone has higher water saturation than the sandstone, presented in Table 2.

Generally, examining the other petrophysical models for the different sequences indicates that the 10At1 sequence has good pore volume and connectivity in the reservoir, and high deliverability of gas is expected.

The surfaces created, indicating the gas water contacts (GWCs) displayed in red colour (Fig. 16a–c) was subsequently used to estimate the gas initially in place. The pink colour in Fig. 16a indicates the position of GWC used to determine the spill points. The GWCs were quality checked and validated by integrating core data, well logs and well completion reports. The GWC for the 13At1 sequence was identified at depth 2580 m, for 10At1 upper sand at depth 2889 m, and that of the lower 10At1 sand at depth 2926 m, used for calculating the initial gas in place.

Another parameter used to estimate the volume of hydrocarbon in place is the bulk rock volume (BRV) that determines the volume and the area of rock above the GWC. In calculating the volume of hydrocarbon (gas) initially in place, the bulk rock volume, net to gross (NTG) ratio, porosity, gas formation volume factor (Bg), and gas saturation of each zones were considered. The volume of gas in place is calculated from Eq. 5 as used by Ma (2018) and Aly (1989):

$$\text{Volume of gas in place (GIIP)} = \frac{\text{BRV} * \text{NTG} * \text{porosity} * (1 - S_w) * \text{constant}}{\text{Gas Formation Volume Factor (Bg)}} \quad (6)$$

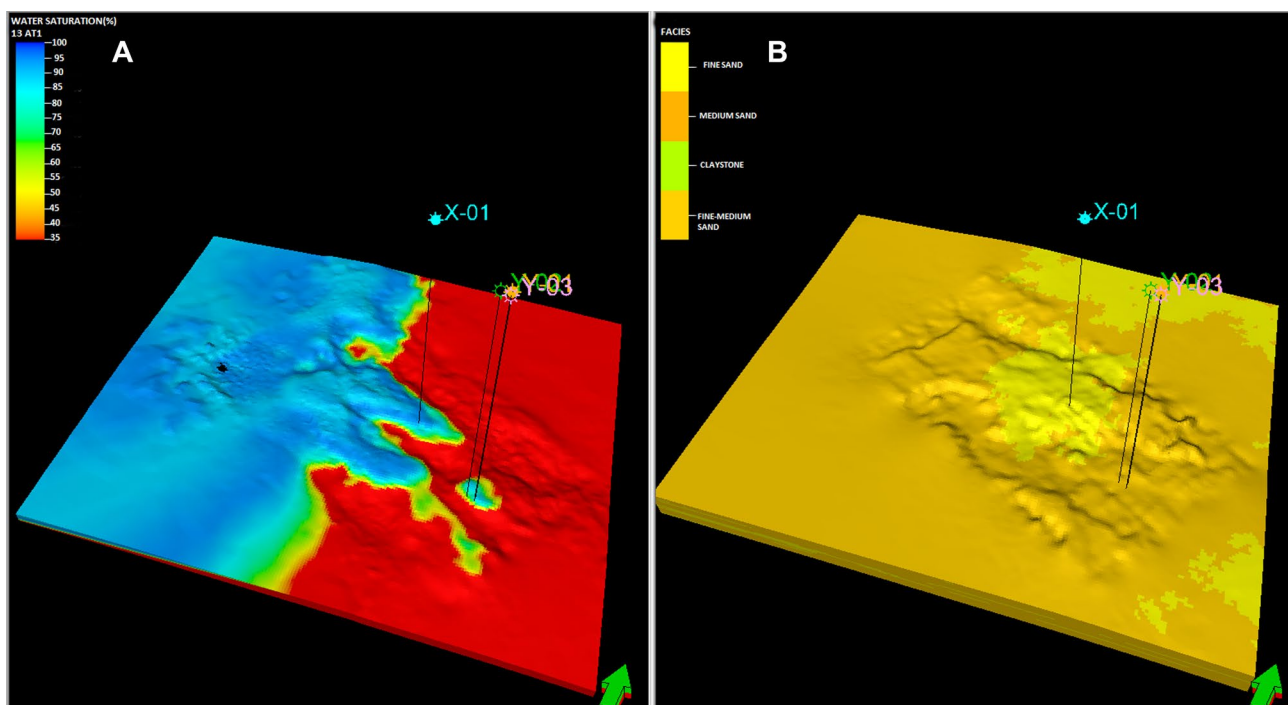


Fig. 15 a, b Results of water saturation model for 13At1. c, d Results of water saturation model for the upper 10At1sand. e, f Results of water saturation model for the lower 10At1 sand

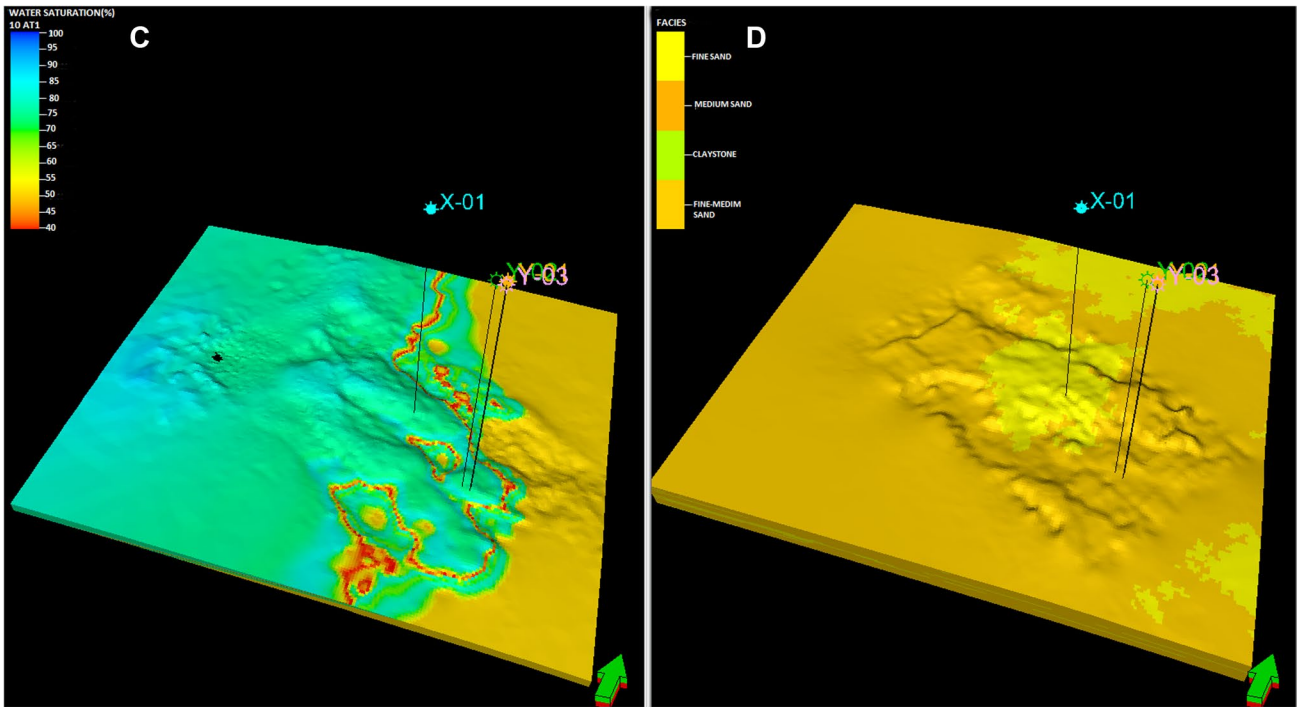


Fig. 15 (continued)

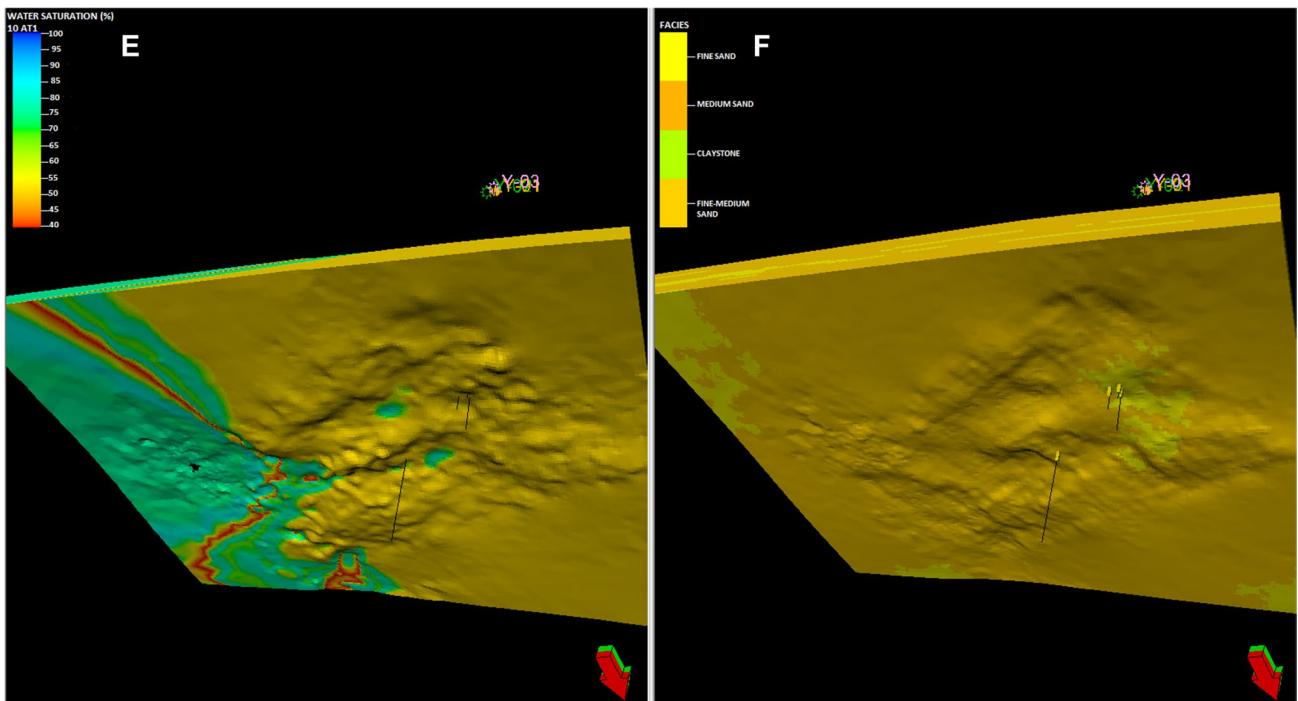


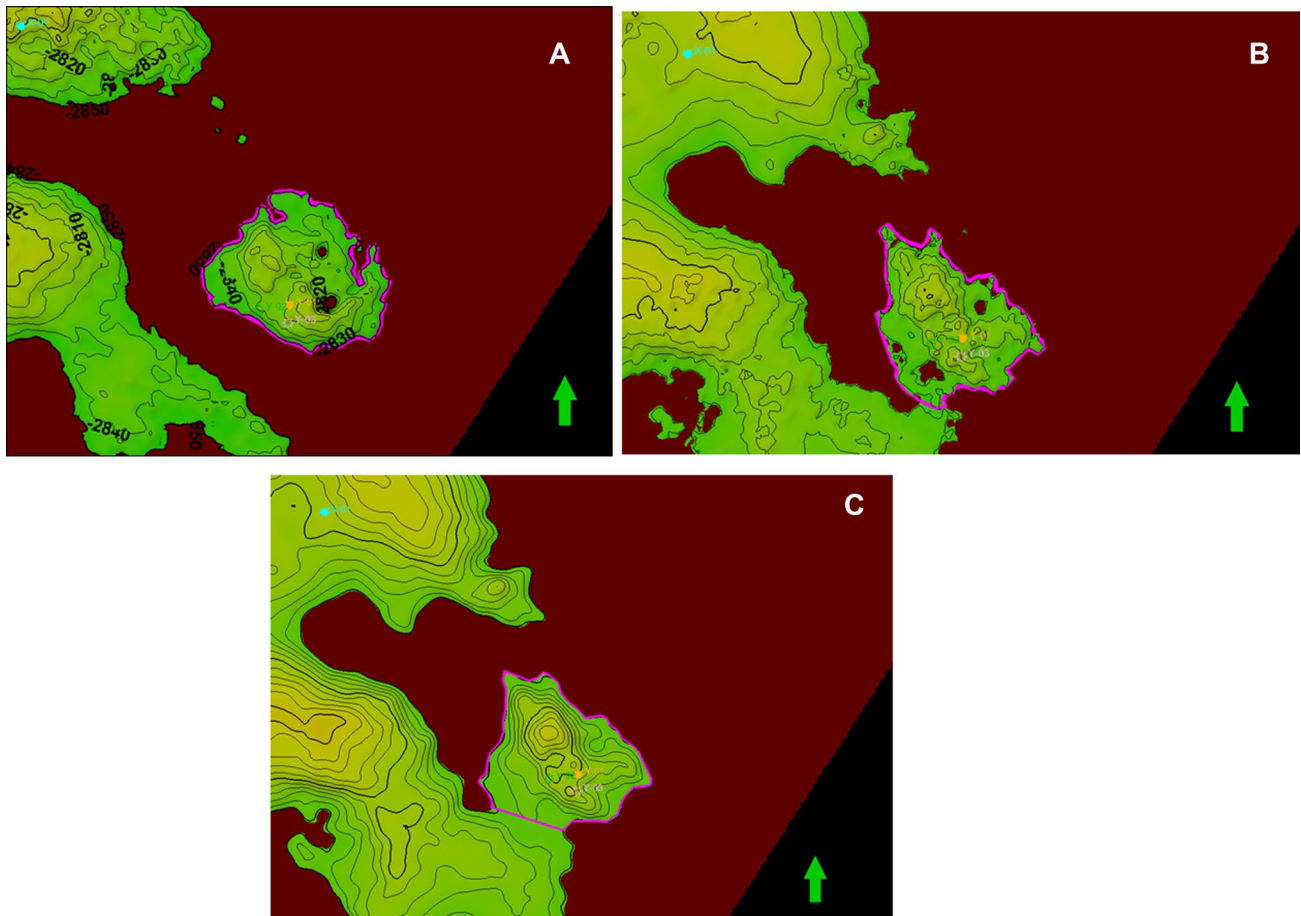
Fig. 15 (continued)

Table 2 A comparison of water saturation values for the different sequences

Sequence	Water saturation %	Average water saturation %
Above 13At1 (claystone)	90–100	95
13At1 sandstone	40–70	45
10At1 sandstone upper	40–65	35
10At1 sandstone lower	20–30	25

The calculation of the volume of gas in place for the various zones (13At1, 10At1 upper, 10At1 lower) sand intervals is presented in Table 3. The 13At1 zone has the most volume of gas, 27.22 bcf, followed by the 10At1 lower with 17.48 bcf, and the 10At1 upper zone with 12.53 bcf, a cumulative 57.23 bcf of gas calculated for all the zones.

The petrophysical parameters (porosity, water saturation and NTG) used to calculate the gas volume in place showed lower uncertainty and more reliability than the Petrel software's results using the core analysis method. For instance, an error in the measurements of the input

**Fig. 16** a-c Position of gas water contact (GWC) used to determine the spill points a for 13 AT1 sand b upper 10At1 sand and c lower 10At1 sand**Table 3** Results of the calculation of the volume of gas in place for the various zones

Zone	GWC (m TVDSS)	BRV (m ³)	NTG	Porosity	Sw	Bg	m ³ to ft ³	GIIP Bcf
13At1	2580	7.20E+07	0.866	0.103	0.400	0.005	35.3147	27.2261
10At1 Upper	2889	4.74E+07	0.734	0.09	0.433	0.005	35.3147	12.53
10At1 Lower	2926	6.03E+07	0.587	0.107	0.347	0.005	35.3147	17.48
Total								57.23

Table 4 Comparison between a study done by PetroSA in 2005 and the current study

2005 Study (PetroSA)		Current study	
Zone	GIIP (Bcf)	Zone	GIIP (Bcf)
13At1	20,54	13At1	27,23
10At1 channel 1	3,37	10At1 upper	12,53
10At1 channel 2	1,33	10At1 lower	17,48
10At1 channel 3	2,42		
Total GIIP of the 10At1 sand	7,12	Total GIIP of the 10At1 sand	30,01
Total GIIP	27,66	Total GIIP	57,23

parameters may result in inaccurate determination of the volume of hydrocarbon. The calibration of log measurements using core measurements reduced uncertainty and enhances the model's reliability by changing the petrophysical input parameters' values that help determine the best parameters that honour the model. The study has demonstrated how 10% error in the petrophysical calculations does not significantly change the initial volume in place results. The results confirm how a threshold within 10% error would not significantly affect the volume calculation results. However, errors higher than 10% in the input parameters would substantially influence the results of volumetric. The bulk or gross rock volume estimated from seismic is indicated as the parameter that may impact volumetric results.

Comparison of the volume in place between PetroSA and current study

The current study is compared with the unpublished in-house study done in 2005 by PetroSA before the seismic was reprocessed. The comparison between the two results is presented in Table 4. The volume in place of the current study differs from the study done in 2005, as different seismic data were used to generate depth maps and ultimately create models used to calculate volumetrics. In the 2005 PetroSA study, the 10At1 sands were divided into three channels. Only the upper and lower sections of the 10At1 sands were identified in the current study. Therefore, both the 13At1 sands and 10At1 sands combined have a higher volume in place in the current study compared to the study conducted in 2005.

The total volume in place has increased by almost twice the previous study. Therefore, it can be concluded that the seismic resolution has improved as mapping of events has become much visible, which increased the volume in place.

Conclusion

The primary purpose of this study was achieved, which is the estimation of the volume of gas in place of the 13At1 and 10At1 sandstones reservoirs deposited in the upper shallow marine environment. Results from this study revealed four facies grouped as facies 1 which is claystone, facies 2 is fine sand, facies 3 is fine-medium sand, and facies 4 is medium sandstone. The medium sandstone has the best reservoir quality, while the claystone has the lowest reservoir quality. This study has produced a calculated volume of gas in the 10At1 sand (upper and lower is 30.01 bcf) higher than that of the 13At1 sand, 27.22 bcf of gas. A total volume of gas in place of 57 bcf was calculated for all the zones evaluated. The depth maps show high structural areas at the 13At1 and 10At1 events. It is advisable to focus further field development in the eastern part of the field because of good reservoir quality and production developed due to the sand in the deeper 10At1 sequence.

Acknowledgements The authors express thanks to the Petroleum Company of South Africa (PetroSA) and the Petroleum Agency of South Africa (PASA) for the data sets used in this study and the permission to publish the results. We also acknowledge the support from Schlumberger for the use of the Petrel Software package.

Funding This research received no specific fund from any funding agency in the public, commercial, or not-for-profit sectors.

Declarations

Conflict of interest Authors have declared that no competing interests exist.

Ethical approval The research does not require any ethical clearance issue.

Open Access This article is licensed under a Creative Commons Attribution 4.0 International License, which permits use, sharing, adaptation, distribution and reproduction in any medium or format, as long as you give appropriate credit to the original author(s) and the source, provide a link to the Creative Commons licence, and indicate if changes were made. The images or other third party material in this article are included in the article's Creative Commons licence, unless indicated otherwise in a credit line to the material. If material is not included in the article's Creative Commons licence and your intended use is not permitted by statutory regulation or exceeds the permitted use, you will need to obtain permission directly from the copyright holder. To view a copy of this licence, visit <http://creativecommons.org/licenses/by/4.0/>.

References

- Ashraf U, Zhu P, Yasin Q, Anees A, Imraz M, Mangi HN, Shakeel S (2019) Classification of reservoir facies using well log and 3D seismic attributes for prospect evaluation and field development: a case study of Sawan gas field, Pakistan. *J Petrol Sci Eng* 175:338–351

- Asquith GB and Gibson CR (1982). Basic relationships of well log interpretation: chapter I, AAPG, Tulsa, USA, 244.
- Atlas D (1979) Log interpretation charts: Houston. Dresser Industries Inc, Texas, p 107
- Bader S, Wu X, Fomel S (2019) Missing log data interpolation and semiautomatic seismic well ties using data matching techniques. *Interpretation* 7:T347–T361
- Baiyegunhi TL, Liu K, Gwavava O, Baiyegunhi C (2020a) Impact of diagenesis on the reservoir properties of the cretaceous sandstones in the southern bredasdorp basin Offshore South Africa. *Minerals* 10:757
- Baiyegunhi TL, Liu K, Gwavava O, Baiyegunhi C (2020b) Petrography and tectonic provenance of the cretaceous sandstones of the bredasdorp basin, off the South coast of South Africa: evidence from framework grain modes. *Geosciences* 10:340
- Baiyegunhi TL, Liu K, Gwavava O, Wagner N, Baiyegunhi C (2020c) Geochemical evaluation of the cretaceous mudrocks and sandstones (Wackes) in the Southern Bredasdorp Basin, Offshore South Africa: implications for hydrocarbon potential. *Minerals* 10:595
- Barton KR, (1997). Delineation of oil and gas fields in the bredasdorp basin, Offshore South Africa, using seismic attribute mapping, seismic inversion and avo techniques, in 5th SAGA biennial conference and exhibition. European Association of Geoscientists & Engineers, p. cp-223.
- Boada, E., Barbato, R., Porras, J.C., Quaglia, A., 2001. Rock typing: key approach for maximizing use of old well log data in mature fields, Santa Rosa field, case study, In: SPE latin american and caribbean petroleum engineering conference. Society of Petroleum Engineers.
- Broad DS, Jungslager EHA, McLachlan IR, Roux J (2006). Offshore mesozoic basins. *The Geology of South Africa*. Geological Society of South Africa, Johannesburg/Council for Geoscience, Pretoria 553, 571.
- Brown LF, (1995). Sequence stratigraphy in offshore south african divergent basins: an atlas on exploration for cretaceous lowstand traps by Soekor (Pty) Ltd, AAPG Studies in Geology 41. AAPG.
- Corbett LW, Frewin J, Barthes C, Kgogo TC, Dubost FX, Navarro R, Tyler E, Portet M, (2011). The use of seismic attributes for depth conversion and property distributions, em field, offshore South Africa, In: SPE EUROPEC/EAGE annual conference and exhibition. Society of Petroleum Engineers.
- Das B, Chatterjee R (2018) Well log data analysis for lithology and fluid identification in Krishna-Godavari Basin India. *Arab J Geosci* 11:231
- Elamri S, Opuwari M, (2016) New insights in the evaluation of reserves of selected wells of the pletmos basin offshore South Africa. Africa Energy and Technology Conference, 2016.
- Elliott T (1997). Brown LF Jr., Benson JM, Brink GJ, Doherty S, Jollands A, Jungslager EHA, Keenan JHG, Muntingh A. & Van Wyk, NJS 1995. Sequence stratigraphy in offshore South African divergent basins. An atlas on exploration for cretaceous lowstand traps by soekor (Pty) Ltd. AAPG studies in geology series no. 41. American Association of Petroleum Geologists ISBN 0 89181 049 8. *Geological Magazine* 134, 121–142.
- Evans AB, Abraham AB, Thompson BE (2019). Integrated reservoir characterisation for petrophysical flow units evaluation and performance prediction. *Open Chem Eng J* 13.
- Fertl WH, Frost E (1980) Evaluation of shaly clastic reservoir rocks. *J Petrol Technol* 32(09):1641–1646
- Gogoi T, Chatterjee R (2019) Estimation of petrophysical parameters using seismic inversion and neural network modeling in upper Assam basin, India. *Geosci Front* 10:1113–1124
- Grobber N, (2005) The Barremian to Aptian gas fairway, Bredasdorp Basin, South Africa, In: 18th world petroleum congress. World Petroleum Congress.
- Gupta SD, Chatterjee R, Farooqui MY (2012) Rock physics template (RPT) analysis of well logs and seismic data for lithology and fluid classification in Cambay Basin. *Int J Earth Sci* 101:1407–1426
- Jungslager EH (1999) Petroleum habitats of the Atlantic margin of South Africa. *Geol Soc, London, Spec Publ* 153:153–168
- Kassab MA, Teama MA, Cheadle BA, El-Din ES, Mohamed IF, Mesbah MA, (2015a). Reservoir characterization of the Lower Abu Madi Formation using core analysis data: El-Wastani gas field, Egypt. *J Afr Earth Sci* 110, 116–130
- Ma ZY (2018) An accurate parametric method for assessing hydrocarbon volumetrics. Revisiting the volumetric equation. *Soc Pet Eng J* 23:1566–1579
- Magoba M, Opuwari M, (2017), An interpretation of core and wireline logs for the Petrophysical evaluation of upper shallow marine sandstone reservoirs of the Bredasdorp Basin, offshore South Africa, In: EGU general assembly conference abstracts. p. 14048.
- McMillan IK, Brink GJ, Broad DS, Maier JJ (1997) Late Mesozoic sedimentary basins off the south coast of South Africa. *Sediment Basins World* 3:319–376
- Miall, AD (1980) Facts and principles of world petroleum occurrence. Canadian Society of Petroleum Geologists.
- Mondal S, Chatterjee R (2021) An integrated approach for characterization in deep-water Krishna -Godavari basin, India: a case study. *J Geophys Eng* 18:134–144
- Mudaly K, Turner J, Escorcial F, Higgs R (2009). FO GasField, Offshore South Africa—an integrated approach to field development. american association of petroleum geologist (AAPG) Search and Discovery Article 20070.
- Nabawy BS, Al-Azazi NA (2015) Reservoir zonation and discrimination using the routine core analyses data: the upper Jurassic Sab'atayn sandstones as a case study, Sab'atayn basin, Yemen. *Arab J Geosci* 8:5511–5530
- Nabawy BS, ElHariri TY (2008) Electric fabric of cretaceous clastic rocks in Abu Gharadig basin, Western desert Egypt. *J Afr Earth Sci* 52:55–61
- Nabawy BS, Rashed MA, Mansour AS, Afify WS (2018) Petrophysical and microfacies analysis as a tool for reservoir rock typing and modeling: rudeis formation, offshore October oil field, sinai. *Mar Pet Geol* 97:260–276
- Neely W, Ismail A, Ibrahim M, Puckette J (2021) Seismic-based characterization of reservoir heterogeneity within the Meramec interval of the STACK play, Central Oklahoma. *Interpretation* 9:T79–T90
- Opuwari M, Kaushalendra BT, Momoh A (2019) Sandstone reservoir zonation using conventional core data: a case study of lower cretaceous sandstones, Orange Basin, South Africa. *J Afr Earth Sc* 153:54–66
- Opuwari M, Amponsah-Dacosta M, Mohammed S, Egesi N (2020a) Delineation of sandstone reservoirs of Pletmos Basin offshore South Africa into flow units using core data. *S Afr J Geol* 2020(123):479–492
- Opuwari, Mimonitu, Mohammed S, Ile C (2020). Determination of reservoir flow units from core data: a case study of the lower cretaceous sandstone reservoirs, western bredasdorp basin offshore in South Africa. *Natural resources research* 1–20.
- Opuwari M, Magoba M, Dominick N, Waldman N (2021). Delineation of sandstone reservoir flow zones in the central bredasdorp basin, South Africa, using core samples. *Natural Resources Research* 1–22.
- Opuwari M (2010). Petrophysical evaluation of the Albian age gas bearing sandstone reservoirs of the OM field, Orange basin, South Africa (PhD Thesis). University of the Western Cape.
- Petroleum Agency SA, (2003). South African Exploration Opportunities. information brochure, South African Agency for Promotion of Petroleum

- Poupon A, Leveaux J (1971) Evaluation of water saturation in shaly formations; Trans. SPWLA 12th Annual Logging Symposium; 2.OnePetro
- Puskarczyk E (2020) Application of multivariate statistical methods and artificial neural network for Facies analysis from well logs data: an example of Miocene deposits. *Energies* 13:1548
- Qassamipour M, Khodapanah E, Tabatabaei-Nezhad SA (2021) A comprehensive method for determining net pay in exploration/development wells. *J Pet Sci Eng* 196:107849
- Radwan AE, Abudeif AM, Attia MM (2020) Investigative petrophysical fingerprint technique using conventional and synthetic logs in siliciclastic reservoirs: A case study, Gulf of Suez basin Egypt. *J Afr Earth Sci* 167:103868
- Roux J (1997) Potential outlined in Southern Outeniqua Basin off South Africa. *Oil & Gas J.* 87–91
- Roux J (2000) The structural development of the southern Outeniqua Basin and dias marginal fracture ridge. *J Afr Earth Sc* 31:64
- Saffou E, Raza A, Gholami R, Croukamp L, Elingou WR, van Bever Donker J, Opuwari M, Manzi MS, Durrheim RJ (2020) Geomechanical characterization of CO₂ storage sites: a case study from a nearly depleted gas field in the Bredasdorp Basin, South Africa. *J Nat Gas Sci Eng* 81:103446
- Sohail GM, Hawkes CD, Yasin Q (2020) An integrated petrophysical and geomechanical characterization of Sembar Shale in the Lower Indus Basin, Pakistan, using well logs and seismic data. *J Nat Gas Sci Eng* 78:103327
- Teama MA, Abuhagaza AA, Kassab MA (2019) Integrated petrographical and petrophysical studies for reservoir characterization of the middle Jurassic rocks at Ras El-Abd, Gulf of Suez, Egypt. *J Afr Earth Sci* 152:36–47
- Turner JR, Grobber N, Sontundu S (2000) Geological modelling of the Aptian and Albian sequences within Block 9, Bredasdorp Basin, offshore South Africa. *J Afr Earth Sci* 31:80
- Van der Spuy D (2003) Aptian source rocks in some South African Cretaceous basins. *Geol Soc, London, Spec Publ* 207:185–202
- Verwer K, Braaksma H (2009). Data report: petrophysical properties of “young” carbonate rocks (Tahiti Reef Tract, French Polynesia), in: *Proc. IODPI Volume.* p. 2.
- White R.E, Simm R (2003). Tutorial: good practice in well ties. first break 21.

Publisher's Note Springer Nature remains neutral with regard to jurisdictional claims in published maps and institutional affiliations.